Supporting Information for

Robust field-free superconducting diode effect in $FeTe_{0.55}Se_{0.45}$

Peng Dong,[1,2,*] Jinghui Wang,[1,2,*] Yanjiang Wang,[1,2] Jianjun Xiao,[1,2] Xiang Zhou,[1,2] Hui Xing,[3] Kenji Watanabe,[4] Takashi Taniguchi,[5] Yueshen Wu,[1,2,†] Yulin Chen,[1,2,6] Jinsheng Wen,[7,‡] and Jun Li[1,2,§]

[1]ShanghaiTech Laboratory for Topological Physics & School of Physical Science and Technology, ShanghaiTech University, Shanghai 201210, China

[2] State Key Laboratory of Quantum Functional Materials, ShanghaiTech University, Shanghai 201210, China

[3]Key Laboratory of Artificial Structures and Quantum Control and Shanghai Center for Complex Physics,
School of Physics and Astronomy, Shanghai Jiao Tong University, Shanghai 200240, China

[4] Research Center for Functional Materials, National Institute for Materials Science, Tsukuba 305-0044, Japan

[5] International Center for Materials Nanoarchitectonics,
National Institute for Materials Science, Tsukuba 305-0044, Japan

[6] Department of Physics, Clarendon Laboratory, University of Oxford, Oxford OX1 3PU, United Kingdom

[7] National Laboratory of Solid State Microstructures and Department of Physics, Nanjing University, Nanjing 210093, China; Collaborative Innovation Center of Advanced Microstructures and Jiangsu Physical Science Research Center, Nanjing University, Nanjing 210093, China

*wuysh@shanghaitech.edu.cn

†jwen@nju.edu.cn

‡lijun3@shanghaitech.edu.cn

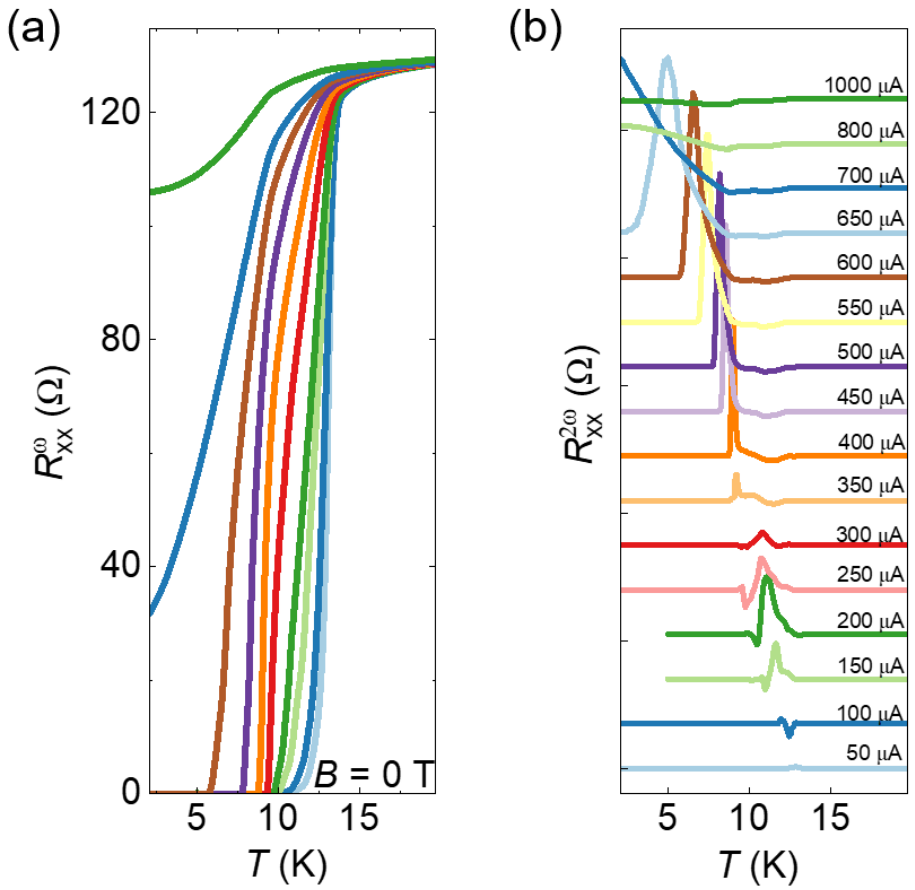

Figure S1| Temperature dependence of both the first (R_{xx}^{ω}) and second ($R_{xx}^{2\omega}$) harmonic resistances under zero magnetic field (0 T) at different current biases. The demagnetization of the PPMS sample chamber was applied by carefully oscillating the field to 0 Oe. As illustrated in Fig. S1(a), the superconducting critical temperature (T_c) was determined at the point where the resistance reaches half its value in the normal state. With low excitation currents, the measured T_c is approximately 13 K. With increasing currents, the superconductivity is progressively suppressed, and the critical current is estimated to be around 1 mA. Fig. S1(b) reveals that the second harmonic resistance ($R_{xx}^{2\omega}$) undergoes a sign reversal. Its magnitude is significantly enhanced with increasing current, eventually reaching the same order of magnitude as the first harmonic resistance (R_{xx}^{ω}). This observation provides compelling evidence for the emergence of substantial time-reversal symmetry breaking or electronic polarization within the system.

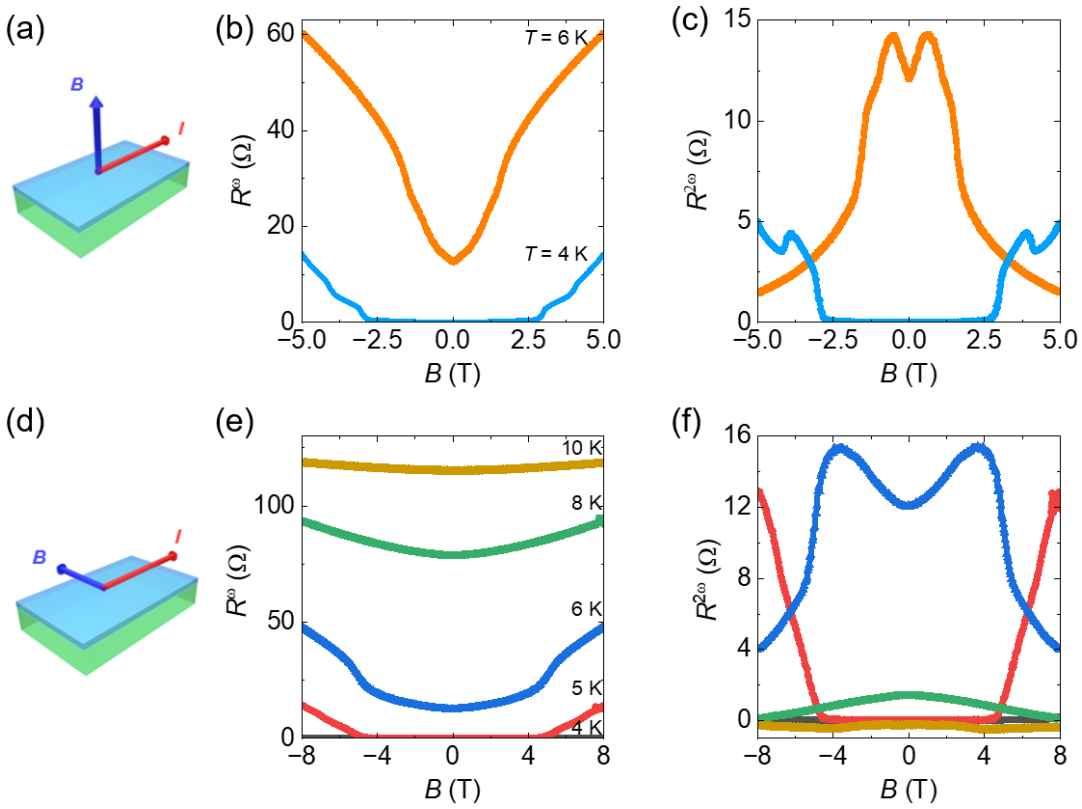

Figure S2| The magnetic field dependence of the first (R_{xx}^{ω}) and second ($R_{xx}^{2\omega}$) harmonic resistances in different temperature when the magnetic field is parallel and perpendicular to current direction at 100 μA. Fig. S2(a) provides a schematic illustration of the current direction and the applied magnetic field, which is oriented perpendicular to both the sample plane and the current. The corresponding first and second harmonic resistances ($R_{xx}^{2\omega}$) are displayed in Figs. S2 (b) and S2 (c). According to the mechanism of magnetic-chiral anisotropy ($R^{2\omega} = R_0\gamma(\boldsymbol{B}\times\boldsymbol{P})\cdot I$), the second harmonic resistance is expected to vanish when the magnetic field is aligned parallel to the direction of symmetry breaking ($\boldsymbol{P}$). Intriguingly, however, a pronounced second harmonic resistance ($R_{xx}^{2\omega}$) emerges within the superconducting transition region, exhibiting an even-symmetric dependence on the magnetic field. This observation suggests a potential and necessary connection to the even-symmetric relationship between the superconducting diode effect and the applied magnetic field. Fig. S2(d) presents a schematic illustration of the magnetic field applied within the sample plane and perpendicular to the current direction. Fig. S2(e) demonstrates the progressive suppression of superconductivity with increasing temperature. Correspondingly, Fig.

S2(f) reveals that the second harmonic resistance exhibits a distinct even-symmetric relationship with the magnetic field, which gradually diminishes as the temperature rises. These findings stand in contradiction to the mechanism of magnetic-chiral anisotropy, which would predict an odd-symmetric dependence, suggesting that the observed nonreciprocal transport in the system may originate from alternative underlying factors.

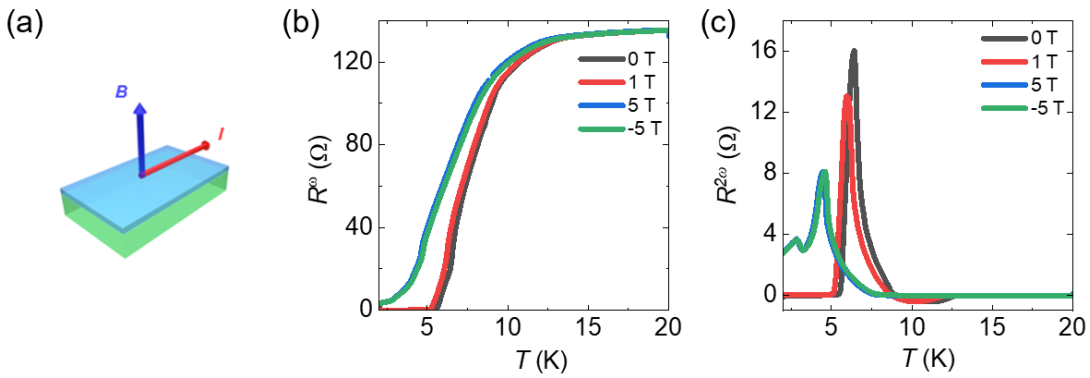

Figure S3| The dependence of the first (R_{xx}^{ω}) and second $(R_{xx}^{2\omega})$ harmonic resistances on temperature under various magnetic fields, with a fixed current bias of 100 μA. Fig.S3 (a) provides a schematic illustration of the magnetic field orientation, which is applied out-of-plane. As shown in Fig.S3 (b), the superconducting state is progressively suppressed with increasing magnetic field strength. Fig.S3 (c) reveals that the second harmonic resistance emerges within the superconducting transition region, reaching its maximum value at zero field and diminishing as the magnetic field intensifies. More notably, the second harmonic resistance $(R_{xx}^{2\omega})$ does not undergo a sign reversal upon inversion of the magnetic field direction, thereby indicating an even-symmetric dependence on the applied magnetic field.

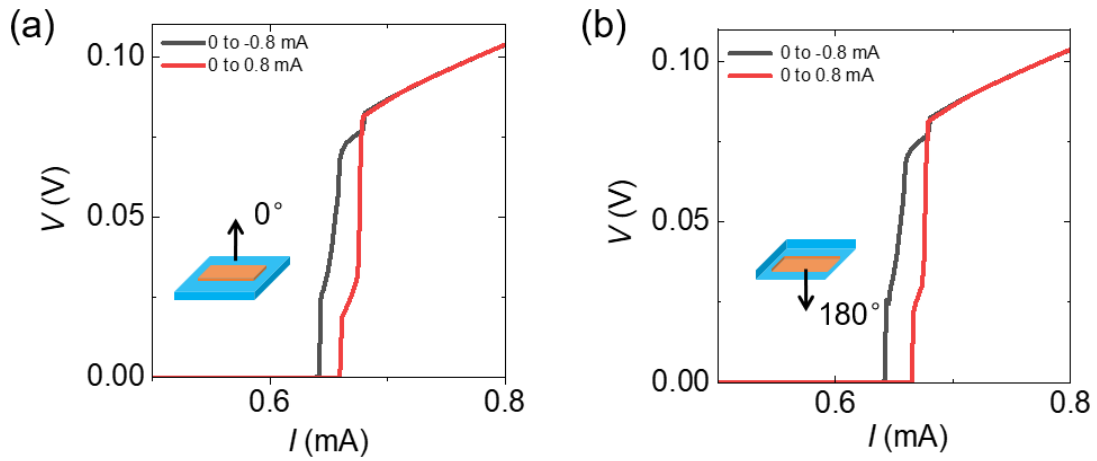

Figure S4| To confirm that the residual field does not affect the diode behavior, the field-free superconducting diode at 2 K of the sample was measured with two orientations of 0° in S4(a) and 180° in S4 (b) by using a rotator stage. The magnetic field of PPMS had been oscillated to 0 Oe before measurements. As the corresponding current-voltage transport characteristics remain unchanged, it is thereby demonstrated that the residual magnetic field has no discernible impact on the superconducting diode effect.

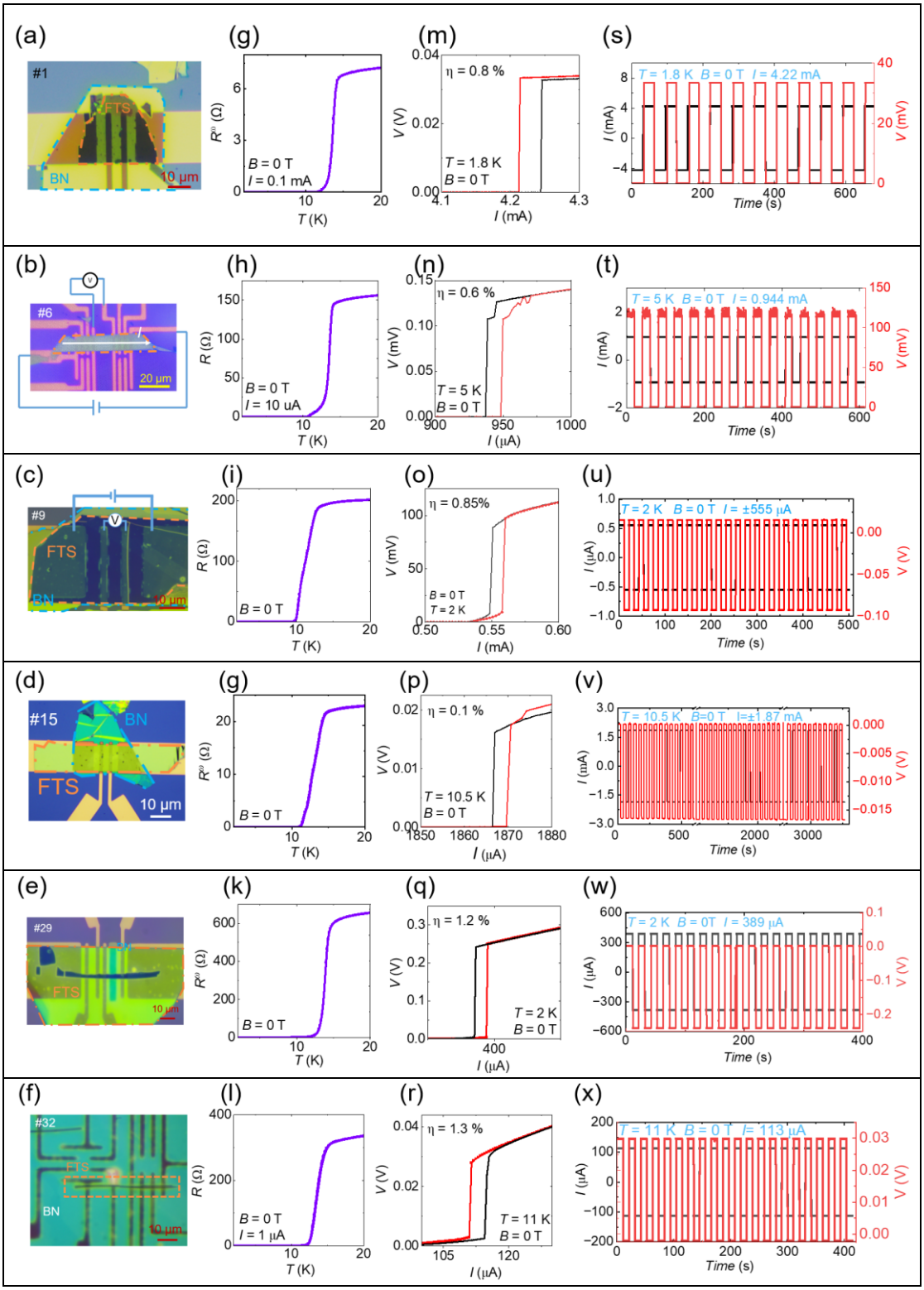

Figure S5| Field-free superconducting diode effect in multiple devices. Fig. (a)-(f) illustrates schematic diagrams of distinct patterned sample structures, fabricated via dry-transfer methodology. Each specimen bears its designated identifier in the upper-left corner, encapsulated within boron nitride for protection. Fig. (g)-(i) present the

temperature dependence of electrical resistance under zero-field conditions, revealing a superconducting transition temperature of approximately 12 K. The current-voltage transport characteristics in the absence of magnetic fields are displayed in Fig. (m)-(r). The black traces denote current sweeps from zero to negative polarity, while red traces represent sweeps from zero to positive polarity, exhibiting pronounced asymmetry. The rectification ratio was quantified accordingly. Fig. (s)-(x) demonstrate zero-field half-wave rectification effects at specified bias currents, and the corresponding rectification coefficients η, was calculated $\frac{|I_c^+ - I_c^-|}{|I_c^+ + I_c^-|} * 100\%$.

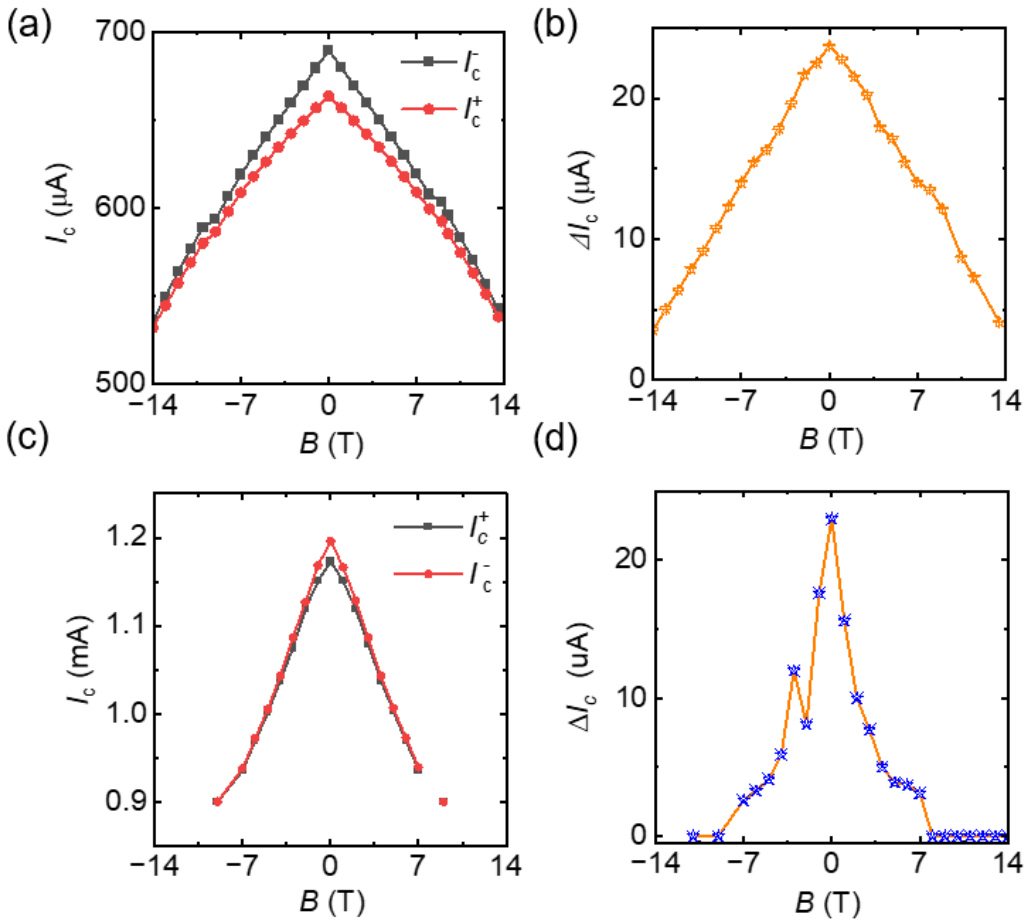

Figure S6| The dependence of forward and reverse critical currents and their differentials on magnetic fields in both regular samples (a)(b) and irregular samples (c)(d), respectively.

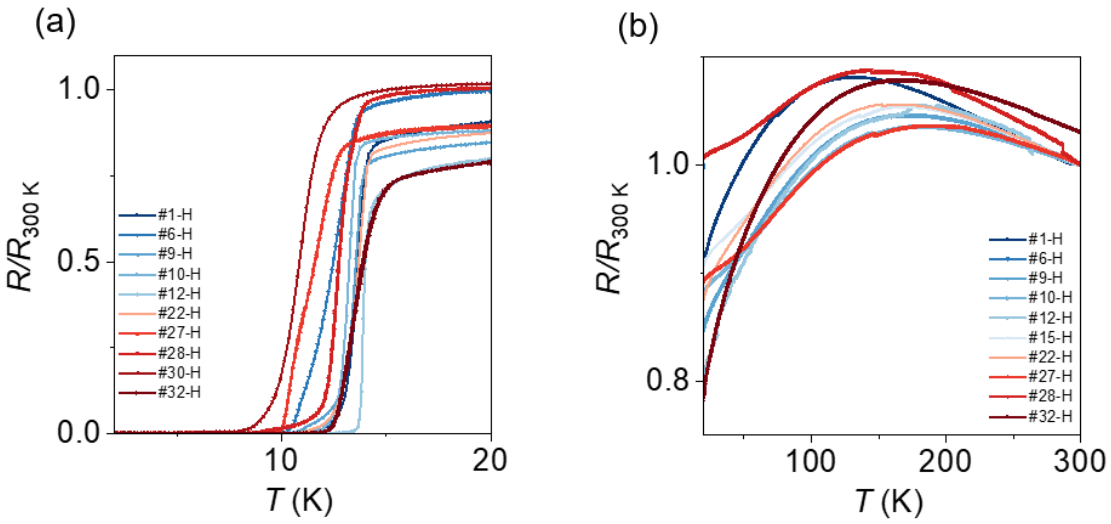

Figure S7| The temperature-dependent resistance in samples manifesting the superconducting diode effect. Notwithstanding nearly identical superconducting transitions in (a), certain devices exhibit a resistivity upturn preceding the transition, while others maintain a more metallic character (b).